A Non-WSSUS Mobile-to-Mobile Channel Model Assuming Velocity Variations of the Mobile Stations

Carlos A. Gutiérrez
Universidad Autónoma
de San Luis Potosí
Faculty of Science
78290 San Luis Potosí, México
Email: cagutierrez@ieee.org

Matthias Pätzold
University of Agder
Faculty of Engineering and Science
NO-4898 Grimstad, Norway
Email: matthias.paetzold@uia.no

Wiem Dahech and Neji Youssef
Université de Carthage
Ecole Supérieure des
Communications de Tunis
2083 EL Ghazala, Ariana, Tunisia
Emails: wiem.dahech@supcom.tn
neji.youssef@supcom.rnu.tn

***Abstract*—This paper aims to characterize the effects that the velocity variations of the mobile stations (MSs) produce on the correlation properties of non-stationary time-frequency (TF) dispersive mobile-to-mobile (M2M) fading channels. Toward that end, we propose a novel geometrical model for non-wide-sense stationary uncorrelated scattering (non-WSSUS) M2M channels that incorporates such variations following a plane wave propagation approach. Capitalizing on the mathematical simplicity of this approach, we derive a general expression for the four-dimensional (4D) TF correlation function (TFCF) of the proposed channel model. From this expression, we analyze the influence of the MSs' acceleration/deceleration on the channel's correlation properties. Some simulation examples illustrating our findings are presented for the particular case of the geometrical one-ring scattering model. The proposed channel model can be used as a reference to study the performance of emerging vehicular communication systems in safety-threatening scenarios, such as when a MS is forced to break suddenly.**

***Keywords*—Accelerated motion, channel modeling, mobile-to-mobile communications, non-stationary processes, non-WSSUS channels, radiowave propagation, vehicular communications.**

I. Introduction

The interest that exists globally in the development of vehicular communication systems for road safety and traffic management applications has opened new research directions in the wireless communications field [1], [2]. One of such directions targets at modeling the non-stationary characteristics of the vehicular communication channel that have been observed empirically. To address this problem, several different geometry-based statistical models (GBSMs) for non-wide-sense stationary uncorrelated scattering (non-WSSUS) mobile-to-mobile (M2M) fading channels have recently been proposed, e.g., see [3]–[6]. An important feature of these models is that they lend themselves to the mathematical analysis of the relevant statistics of non-stationary channels, such as the correlation and scattering functions. However, a review of the literature reveals that the existing GBSM for non-WSSUS M2M channels have been formulated by assuming constant velocities of the transmitting and receiveing mobile stations (MSs). This assumption is reasonably justified in many situations in which the vehicular communication systems are expected to operate. Nevertheless, an acceleration/deceleration component should be included to properly characterize the channel's dynamics for important scenarios that arise occasionally, such as when a vehicle accelerates in preparation to overtake a slower one, or when a vehicle brakes suddenly.

To close the gap, we propose in this paper a novel GBSM for non-WSSUS M2M fading channels that incorporates velocity variations of the MSs. The proposed model has been formulated following a plane wave propagation approach that facilitates the characterization of the channel's nonstationarities stemming from the propagation over small local areas. Capitalizing on the mathematical simplicity of this approach, we derive a general expression for the channel four-dimensional (4D) time-frequency correlation function (TFCF). To the best of the authors' knowledge, the effects produced by the MSs' acceleration/deceleration on the correlation properties of non-WSSUS channel have not been analytically investigated before. However, a closely related work is presented in [7]. In that paper, the authors characterize the correlation and spectral properties of non-stationary narrowband M2M channels assuming variations in the MSs' speeds and trajectories. The main difference between our work and that in [7] is that we are dealing here with the modeling of non-stationary doubly-selective M2M channels, whereas the focus of [7] is only on time-selective channel characteristics. Another important difference is that the motion of the MSs is characterized in this paper by the sum of a velocity vector and an acceleration vector. By contrast, the model of motion considered in [7] cannot be expressed as the sum of such vectors. Finally, the authors of [7] assume that each "echo" of the transmitted signal interacts with two different interfering objects (IOs) before impinging on the receiver antenna. In this paper, we suppose that each propagation path expriences only a single interaction with IOs.

The remainder of the paper is organized in four sections: Our proposal for the geometrical modeling of non-WSSUS M2M fading channels assuming variations in the MSs' velocities is presented in Section II. The 4D TFCF of the proposed channel model is analyzed in Section III. Some numerical examples illustrating our findings are presented in Section IV for the particular case of the geometrical one-ring scattering model. Finally, our conclusions are given in Section V.

Notation: The complex conjugate and the absolute value operations are denoted by $(\cdot)^*$ and $|\cdot|$, respectively. Vectors are written in bold-face. The transpose operation is denoted by $(\cdot)^\dagger$, $\|\cdot\|$ stands for the Euclidean norm, and the scalar product between two vectors $\mathbf{z}_1$ and $\mathbf{z}_2$ is represented as $\langle \mathbf{z}_1, \mathbf{z}_2 \rangle$. The operator $\mathcal{E}\{\cdot\}$ designates the statistical expectation. The set of positive real numbers is denoted by $\mathbb{R}^+$.

II. The Proposed GBSM for Non-WSSUS M2M Channels

A. Mathematical Model of the Channel Impulse Response

The scope of this paper is on the characterization of small-scale non-WSSUS channels for single-input single-output (SISO) M2M communication systems. We assume that multiple replicas of the transmitted signal arrive at the receiver via a single interaction with IOs that are static and arbitrarily located on the propagation environment. Under this condition, we define the baseband-equivalent channel impulse response (CIR) at time t due to an impulse applied τ seconds in the past by the superposition of $\mathcal{L}$ electromagnetic plane waves as

$$h(t;\tau) \triangleq \Pi_{T_0}(t) \sum_{\ell=1}^{\mathcal{L}} g_\ell \exp\left\{j\varphi_\ell(t)\right\} \delta(\tau - \tau_\ell(t)) \quad (1)$$

where $j^2 = -1$, $\delta(\cdot)$ is the Dirac delta function, g_ℓ is an attenuation factor introduced by the interaction of the transmitted signal with the ℓth IO; $\varphi_\ell(t)$ and $\tau_\ell(t)$ are the instantaneous phase and propagation delay of the ℓth received electromagnetic wave, respectively, and $\Pi_{T_0}(t)$ is a windowing function given by

$$\Pi_{T_0}(t) \triangleq \begin{cases} 1, & 0 \le t \le T_0 \\ 0, & \text{otherwise.} \end{cases} \quad (2)$$

The windowing function is introduced as a means to limit the length of the CIR $h(t;\tau)$ within an interval of length T_0 inside of which the large-scale variations of the channel are negligible. The instantaneous phase $\varphi_\ell(t)$ of the ℓth received plane wave can be modeled as

$$\varphi_\ell(t) = \theta_0 - \theta_\ell - \vartheta_\ell^T(t) - \vartheta_\ell^R(t) \quad (3)$$

where θ_0 is the initial phase of the transmitted signal, θ_ℓ is a phase rotation produced by the interaction with the ℓth IO, $\vartheta_\ell^T(t)$ and $\vartheta_\ell^R(t)$ are additional phase rotations related to the distance that the ℓth received wave travels from the transmitting MS (T_X) to the ℓth IO, and from there to the receiving MS (R_X), respectively. Without loss of generality, we will henceforth assume that $\theta_0 = 0$.

B. Geometrical Modeling of the CIR Parameters

For the characterization of the instantaneous propagation delay $\tau_\ell(t)$, and phase rotations $\vartheta_\ell^T(t)$ and $\vartheta_\ell^R(t)$, we will consider an arbitrary geometrical configuration of the propagation area, such as the one illustrated in Fig. 1. The IOs are represented in Fig. 1 by black dots. The time-invariant vector $\mathbf{s}_\ell$ indicates the position of the ℓth IO. In turn, $\mathbf{p}_0^T$ and $\mathbf{p}_0^R$ stand for the initial position of T_X and R_X, respectively,

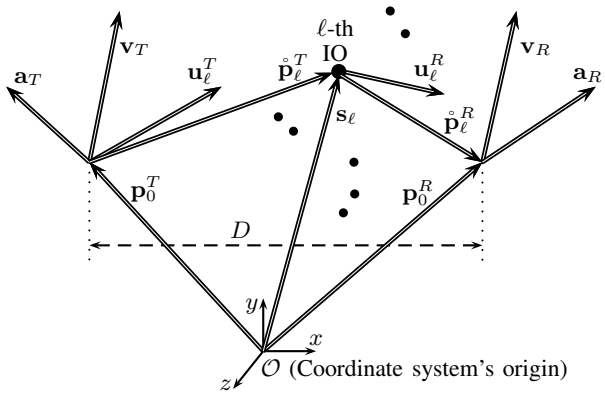

Fig. 1. The reference 2D propagation scenario at time $t_0 = 0$.

i.e., the position of the MSs at the time $t = 0$ when the communications between them begin. The distance between $\mathbf{p}_0^T$ and $\mathbf{p}_0^R$ is equal to D, that is, $\|\mathbf{p}_0^T - \mathbf{p}_0^R\| = D$. The initial velocities of T_X and R_X are given by the vectors $\mathbf{v}_T$ and $\mathbf{v}_R$, respectively, while the corresponding acceleration vectors are denoted by $\mathbf{a}_T$ and $\mathbf{a}_R$. The time-invariant vectors $\mathring{\mathbf{p}}_\ell^T$ and $\mathring{\mathbf{p}}_\ell^R$ indicate, in that order, the position of the ℓth IO as seen from the initial position of T_X, and the initial position of R_X as seen from the ℓth IO. Note that $\mathring{\mathbf{p}}_\ell^T = \mathbf{s}_\ell - \mathbf{p}_0^T$, and $\mathring{\mathbf{p}}_\ell^R = \mathbf{p}_0^R - \mathbf{s}_\ell$. Finally, $\mathbf{u}_\ell^T$ and $\mathbf{u}_\ell^R$ are unit vectors that point in the direction of propagation of the ℓth received wave on transmission and after the interaction with the ℓth IO, respectively.

Following the geometrical channel modeling approach presented in [5], [6], and with reference to Fig. 1, we define the propagation delay $\tau_\ell(t)$ and the phases $\vartheta_\ell^T(t)$ and $\vartheta_\ell^R(t)$ as

$$\vartheta_\ell^T(t) \triangleq \kappa_0 \langle \mathbf{p}_\ell^T(t), \mathbf{u}_\ell^T \rangle \quad (4)$$

$$\vartheta_\ell^R(t) \triangleq \kappa_0 \langle \mathbf{p}_\ell^R(t), \mathbf{u}_\ell^R \rangle \quad (5)$$

$$\tau_\ell(t) \triangleq \frac{\langle \mathbf{p}_\ell^T(t), \mathbf{u}_\ell^T \rangle + \langle \mathbf{p}_\ell^R(t), \mathbf{u}_\ell^R \rangle}{\mathcal{C}} \quad (6)$$

where $\kappa_0 = 2\pi/\lambda$ is the wavenumber of the transmitted signal, λ stands for the wavelength, and $\mathcal{C}$ is the speed of light. The time-varying vector $\mathbf{p}_\ell^T(t)$ indicates the position of the ℓth IO with respect to (w.r.t.) the instantaneous position of T_X, whereas $\mathbf{p}_\ell^R(t)$ describes the instantaneous position of R_X as seen from the ℓth IO. Regardless of how the IOs are arranged, the instantaneous position vectors $\mathbf{p}_\ell^T(t)$ and $\mathbf{p}_\ell^R(t)$ can be written as

$$\mathbf{p}_\ell^k(t) = \mathring{\mathbf{p}}_\ell^k - c_k \mathbf{m}_k(t), \quad k \in \{T, R\} \quad (7)$$

where $c_k = 1$ if $k = T$, and $c_k = -1$ if $k = R$. The time-varying vector $\mathbf{m}_k(t)$, $k \in \{T, R\}$, accounts for the motion of T_X ($k = T$) and R_X ($k = R$). From classical mechanics, and assuming constant acceleration, we can define

$$\mathbf{m}_k(t) = t\left(\mathbf{v}_k + \frac{1}{2} t \cdot \mathbf{a}_k\right), \quad k \in \{T, R\}. \quad (8)$$

The model of motion defined above is similar to the one considered in [7] in the sense that both models can be used to describe motion over linear and curvilinear trajectories.

However, the model in (8) applies for trajectories over open curves, such as parabolic and hyperbolic curves, while the model in [7] is valid for curvilinear trajectories over circles and spirals.

The M2M channel model given by (1)–(8) is transparent to the geometrical configuration of the IOs' location, and is valid regardless of whether the vectors that characterize the relative position among IOs and MSs are defined in a two-dimensional (2D) or a three-dimensional (3D) space. However, to simplify our analysis, we will restrict our attention to the case of a 2D propagation scenario. For this particular case, the parameters of the velocity, acceleration, and position vectors introduced in this section will be defined as in Table I, where the notation $\mathbf{x} = M_x \angle \Theta_x$ indicates that $\mathbf{x}$ is a vector having a magnitude M_x and a direction specified by the angle Θ_x. The angles ϕ_ℓ^T and ϕ_ℓ^R presented in Table I can be identified as the angle of departure (AOD) and angle of arrival (AOA), respectively, of the ℓth received plane wave. The interpretation of the other vector parameters is in analogy to the definition of the corresponding vector.

The AOD ϕ_ℓ^T and AOA ϕ_ℓ^R of the ℓth received plane wave can be modeled in a number of ways. In this paper, we assume that ϕ_ℓ^T and ϕ_ℓ^R are given in such a way that

$$\langle \mathring{\mathbf{p}}_\ell^k, \mathbf{u}_\ell^k \rangle \quad = \quad d_\ell^k, \qquad \text{for } k \in \{T, R\} \tag{9a}$$

meaning that $\mathring{\mathbf{p}}_\ell^k$ and $\mathbf{u}_\ell^k$ are collinear vectors. Under this condition, we find by evaluating (4)–(6) that:

$$\vartheta_\ell^k(t) \quad = \quad \kappa_0\, d_\ell^k - 2\pi t \left[\frac{\dot{f}_{\max}^k(t)}{2} \cos(\phi_\ell^k - \beta_k) + f_{\max}^k \cos(\phi_\ell^k - \gamma_k) \right], \quad \text{for } k \in \{T, R\} \tag{10}$$

$$\tau_\ell(t) \quad = \quad \frac{d_\ell^T + d_\ell^R}{\mathcal{C}} - \frac{t}{f_c} \left[f_\ell^S + \frac{\dot{f}_\ell^A(t)}{2} \right] \tag{11}$$

where $f_{\max}^k = \nu_k/\lambda$, $\dot{f}_{\max}^k(t) = t \cdot a_k/\lambda$, for $k \in \{T, R\}$, $f_c = \mathcal{C}/\lambda$ is the carrier frequency, and

$$f_\ell^S \quad = \quad f_{\max}^T \cos(\phi_\ell^T - \gamma_T) + f_{\max}^R \cos(\phi_\ell^R - \gamma_R) \tag{12}$$

$$\dot{f}_\ell^A(t) \quad = \quad \dot{f}_{\max}^T(t) \cos(\phi_\ell^T - \beta_T) + \dot{f}_{\max}^R(t) \cos(\phi_\ell^R - \beta_R). \tag{13}$$

The parameters f_ℓ^S and $\dot{f}_\ell^A(t)$ characterize the Doppler frequency shifts caused by the MSs' speed and acceleration, respectively. Note that if the AODs ϕ_ℓ^T and AOAs ϕ_ℓ^R are modeled by random variables, then the time-invariant Doppler frequencies f_ℓ^S are random variables too, whereas the time-varying Doppler frequencies $\dot{f}_\ell^A(t)$ are stochastic processes.

C. Modeling of the Instantaneous Doppler Shift

The instantaneous Doppler frequency shift $\upsilon_\ell^D(t)$ of the ℓth received plane wave can be computed from the time-varying phase $\varphi_\ell(t)$ as [8]

$$\upsilon_\ell^D(t) \quad = \quad \frac{1}{2\pi} \frac{d\varphi_\ell(t)}{dt}. \tag{14}$$

TABLE I
VECTORS THAT CHARACTERIZE THE RELATIVE POSITIONS AMONG IOS AND MSS

Vector	Form
Velocity vector of T_X	$\mathbf{v}_T = \nu_T \angle \gamma_T$
Velocity vector of R_X	$\mathbf{v}_R = \nu_R \angle \gamma_R$
Acceleration vector of T_X	$\mathbf{a}_T = a_T \angle \beta_T$
Acceleration vector of R_X	$\mathbf{a}_R = a_R \angle \beta_R$
Position of the ℓth scatterer w.r.t. the initial position of T_X	$\mathring{\mathbf{p}}_\ell^T = d_\ell^T \angle \alpha_\ell^T$
Initial position of R_X as seen from the ℓth scatterer	$\mathring{\mathbf{p}}_\ell^R = d_\ell^R \angle \alpha_\ell^R$
Unit vector pointing at the direction of propagation of the plane wave that travels from T_X to the ℓth scatterer	$\mathbf{u}_\ell^T = 1 \angle \phi_\ell^T$
Unit vector pointing at the direction of propagation of the plane wave that travels from the ℓth scatterer to R_X	$\mathbf{u}_\ell^R = 1 \angle (\phi_\ell^R + \pi)$

From the results presented in (3) and (10), one can easily verify that

$$\upsilon_\ell^D(t) \quad = \quad f_\ell^S + \dot{f}_\ell^A(t), \quad \forall \ell. \tag{15}$$

The equation above is different from the one obtained in [7]. This was to be expected, since the underlying models of motion of the MSs are different.

III. Correlation Properties of the Proposed Model for Non-WSSUS M2M Channels

A. Definitions and Considerations

The 4D TFCF of the non-WSSUS channel is defined as

$$R_H(t, f; \Delta t, \Delta f) \;\triangleq\; \mathcal{E}\{H^*(t - \Delta t; f) H(t; f + \Delta f)\} \tag{16}$$

where

$$H(t; f) \triangleq \int_{-\infty}^{\infty} h(t; \tau) \exp\{-j2\pi f \tau\} d\tau \tag{17}$$

$$= \Pi_{T_0}(t) \sum_{\ell=1}^{\mathcal{L}} g_\ell \exp\big\{ -j\big[\theta_\ell + 2\pi \tau_\ell(t)[f_c + f]\big]\big\} \tag{18}$$

is the channel transfer function. For the evaluation of (16), we will assume that the interaction with the IOs produces a random attenuation and a random phase shift on the impinging electromagnetic waves. With this in mind, we characterize the gains g_ℓ by statistical independent, but not necessarily identically distributed, positive random variables. We assume that the average power of the gains is given in such a way that $\sum_{\ell=1}^{\mathcal{L}} \mathcal{E}\{|g_\ell^2|\} = \sigma_h^2$, where σ_h^2 is the average power of the channel. Furthermore, we model the phases θ_ℓ by random variables uniformly distributed over $[-\pi, \pi)$.

In order to obtain a general expression of $R_H(t, f; \Delta t, \Delta f)$ that is not restricted to any particular geometrical configuration of the propagation area, we characterize the distances d_ℓ^T and

d_ℓ^R introduced in Table I as functions of the AODs ϕ_ℓ^T and AOAs ϕ_ℓ^R, that is:

$$d_\ell^T = \mathcal{G}_T(\phi_\ell^T), \qquad \mathcal{G}_T : [-\pi, \pi) \longmapsto \mathbb{R}^+ \tag{19a}$$

$$d_\ell^R = \mathcal{G}_R(\phi_\ell^R), \qquad \mathcal{G}_R : [-\pi, \pi) \longmapsto \mathbb{R}^+. \tag{19b}$$

We assume that the local scatterers are distributed randomly around the receiver. The AOAs ϕ_ℓ^R can therefore be modeled by independent and identically distributed (i.i.d.) random variables characterized by a circular probability density function (PDF) $p_\phi^R(\phi)$. Without loss of generality, we will consider that the initial position vectors $\mathbf{p}_0^T$ and $\mathbf{p}_0^R$ are aligned with the coordinate system's x-axis, in such a way that $\mathring{\mathbf{p}}_\ell^T = [D, 0] - \mathring{\mathbf{p}}_\ell^R$. Hence, the AODs ϕ_ℓ^T can be written as follows

$$\phi_\ell^T = \arctan\left(\frac{d_\ell^R \sin(\phi_\ell^R)}{D + d_\ell^R \cos(\phi_\ell^R)}\right), \quad \forall \ell. \tag{20}$$

Finally, we will assume that the gains g_ℓ, the phases θ_ℓ, and the AOAs ϕ_ℓ^R are mutually independent for all ℓ.

B. General Solution of the 4D TFCF of the Proposed Geometrical Model for Non-WSSUS M2M Channels

From (16) and (17), we have

$$R_H(t, f; \Delta t, \Delta f) = \sigma_h^2 \, \Upsilon_{T_0}(t, \Delta t) \times \mathcal{E}\left\{ \exp\left\{ j2\pi \Big[\big(f_c + f\big)\big[\tau(t - \Delta t) - \tau(t)\big] - \Delta f \tau(t) \Big] \right\} \right\} \tag{21}$$

where $\Upsilon_{T_0}(t, \Delta t) = \Pi_{T_0}(t) \, \Pi_{T_0}(t - \Delta t)$, and

$$\tau(t) = \frac{\mathcal{G}_T(\phi_T) + \mathcal{G}_R(\phi_R)}{\mathcal{C}} - \frac{t}{f_c}\left[f_S + \frac{\dot{f}_A(t)}{2} \right]. \tag{22}$$

In the previous equation, ϕ_R is an arbitrary AOA in the set $\{\phi_1^R, \phi_2^R, \ldots, \phi_{\mathcal{L}}^R\}$, and f_S, $\dot{f}_A(t)$, and ϕ_T are functions of ϕ_R given as in (12), (13), and (20), respectively. Substituting (22) into (21), and invoking the expected value theorem [9], we obtain the general solution presented in (23) at the bottom of this page. Details on the derivations are omitted for reasons of brevity.

C. Discussion of Results

From (23), we can observe that the 4D TFCF of $H(t; f)$ is a TF-dependent function, meaning that $R_H(t_1, f_1; \Delta t, \Delta f) \neq R_H(t_2, f_2; \Delta t, \Delta f)$ for $(t_1, f_1) \neq (t_2, f_2)$. The proposed channel model is therefore a 2D random process that does not fulfill the WSSUS condition. It is worth highlighting that the nonstationarities of our channel model are not caused by factors typically associated with non-stationary channels, such as a time-varying average power due to path loss or shadowing, or time-shift sensitive correlation properties due to gross changes of the IOs (appearance and disappearance of scattering and reflecting objects). The nonstationarities of our channel model stem, on the one hand, from the time-varying nature of the propagation delays, and on the other hand, from the accelerated motion of the MSs. Each of these two factors is by itself a source for nonstationarities, as one may observe from (23) by making either $\dot{f}_A(t) = 0$, or $\Delta f = 0$.

The special case of non-accelerated linear motion of the MSs, which ensues when $\dot{f}_A(t) = 0$, is analyzed in detail in [6]. The results presented in that paper indicate that the WSSUS condition is not compatible with the time-varying nature of the propagation delays, implying that the wide-sense stationary (WSS) condition cannot be met simultaneously in the time and the frequency domains. However, such results suggest that if the frequency selectivity of $H(t; f)$ is neglected (i.e., if $\Delta f = 0$), assuming, e.g., a communication system operating with a very narrow bandwidth, then the WSS condition is fulfilled in the time domain. This is not the case if the MSs' motion includes an acceleration component, since the 4D TFCF in (23) still is a TF-dependent function if we neglect the frequency selectivity of $H(t; f)$ and $\dot{f}_A(t) \neq 0$. This is consistent with the work of previous papers that investigate the stationary characteristics of frequency-nonselective multipath fading channels under conditions of accelerated motion of the MSs, e.g., see [7]. On the other hand, the results obtained in [6] indicate that if the channel's time selectivity is neglected, i.e., if $\Delta t = 0$, then $H(t; f)$ can be characterized by a frequency-domain WSS random process. The expression in (23) shows that this remark also applies under conditions of accelerated motion of the MSs. Note that $R_H(t, f; \Delta t, \Delta f)$ is a frequency-invariant function if we make $\Delta t = 0$ in (23), regardless of the value of $\dot{f}_A(t)$. Aside from these two particular cases, we can conclude from (23) that the acceleration of the MSs exacerbates the nonstationarities of doubly-selective M2M fading channels; particularly those nonstationarities observed in the time domain.

IV. Numerical Examples

In what follows, we will present some numerical examples illustrating the remarks of Section III-C. For that purpose, we will consider the particular case of the geometrical one-ring scattering model [10]. For this geometrical configuration of the propagation area, the functions $\mathcal{G}_T(\phi_\ell^T)$ and $\mathcal{G}_R(\phi_\ell^R)$

$$R_H(t, f; \Delta t, \Delta f) = \sigma_h^2 \, \Upsilon_{T_0}(t, \Delta t) \int_{-\pi}^{\pi} \exp\left\{ j2\pi \left[\frac{f_c + f}{f_c} \left[\frac{\dot{f}_A(\Delta t)}{2}(t - \Delta t) + \Delta t \left(f_S + \frac{\dot{f}_A(t)}{2} \right) \right] - \Delta f \left[\frac{\mathcal{G}_T(\phi_T) + \mathcal{G}_R(\phi)}{\mathcal{C}} - \frac{t}{f_c}\left(f_S + \frac{\dot{f}_A(t)}{2} \right) \right] \right] \right\} p_\phi^R(\phi) d\phi. \tag{23}$$

describing the distance to $\mathbf{s}_\ell$ from $\mathbf{p}_0^T$ and $\mathbf{p}_0^R$, respectively (see Fig. 1), are equal to

$$\mathcal{G}_T(\phi_\ell^T) = \sqrt{D^2 + d^2 - 2dD\cos(\phi_\ell^R)} \quad (24)$$

$$\mathcal{G}_R(\phi_\ell^R) = d \quad (25)$$

for all $\ell = 1, 2, \ldots, \mathcal{L}$, where d is the radius of the ring on which the IOs are located. We will assume also that the statistics of the AOA follow the von Mises distribution with mean $\mu \in [-\pi, \pi)$ and concentration parameter κ, $0 \leq \kappa < \infty$ [10], in such a way that $p_\phi^R(\phi) = \exp\{\kappa\cos(\phi - \mu)\}/(2\pi I_0(\kappa))$, $\phi \in [-\pi, \pi)$, where $I_0(\cdot)$ is the modified Bessel function of the first kind and zeroth order.

Assuming that $d \ll D$, the integral in (23) can be written in a closed form as follows

$$R_H(t, f; \Delta t, \Delta f) \approx \Upsilon(t, \Delta t)\frac{\exp\{j2\pi\mathcal{A}(t, f; \Delta t, \Delta f)\}}{I_0(\kappa)} \times I_0\Bigg(\Big\{\big[\kappa\cos(\mu) + j2\pi\mathcal{B}_c(t, f; \Delta t, \Delta f)\big]^2 + \big[\kappa\sin(\mu) + j2\pi\mathcal{B}_s(t, f; \Delta t, \Delta f)\big]^2\Big\}^{1/2}\Bigg). \quad (26)$$

The functions $\mathcal{A}(t, f; \Delta t, \Delta f)$, $\mathcal{B}_c(t, f; \Delta t, \Delta f)$, and $\mathcal{B}_s(t, f; \Delta t, \Delta f)$ are defined as in (27) at the bottom of this page, where

$$\mathcal{Z}(t, f; \Delta t, \Delta f) = \Delta t\left(\frac{f_c + f}{f_c}\right) + \Delta f\frac{t}{f_c} \quad (28)$$

$$\mathcal{W}(t, f; \Delta t) = \left(\frac{t - \Delta t}{2}\right)\left(\frac{f_c + f}{f_c}\right) \quad (29)$$

$$F_c^k(t) = f_{\max}^k\cos(\gamma_k) + \frac{\dot{f}_{\max}^k(t)}{2}\cos(\beta_k) \quad (30)$$

$$F_s^k(t) = f_{\max}^k\sin(\gamma_k) + \frac{\dot{f}_{\max}^k(t)}{2}\sin(\beta_k) \quad (31)$$

for $k \in \{T, R\}$.

For the simulations, we will consider an observation time window of length $T_0 = 6.4$ ms ($t \in [0, T_0]$), which corresponds to the duration of a long data frame in the IEEE 802.11p standard [2], a carrier frequency $f_c = 5.9$ GHz, and a system bandwidth $B = 10$ MHz ($f \in [-B, B]$). We also set: $\nu_T = 90$ m/s ($f_{\max}^T = 492.01$ Hz), $\nu_R = 70$ m/s ($f_{\max}^R = 382.68$ Hz), $\gamma_T = \beta_T = 105°$, $\gamma_R = 70°$, $\beta_R = 250°$, $a_T = 30$ m/s^2, $a_R = 10$ m/s^2, $D = 300$ m, $d = 30$ m, $\sigma_h^2 = 1$, $\kappa = 1$, and $\mu = 40°$. This choice of parameters describes an arbitrary scenario where R_X is decelerating, while T_X is accelerating and changing lanes in preparation to overtake R_X.

Plots of the 3D-surface and the contour of the absolute value of $R_H(t, f; \Delta t, \Delta f)$ are shown in Fig. 2 for $(t, f) = (0.5T_0, 0.25B)$. We can observe from these two plots that $|R_H(t, f; \Delta t, \Delta f)|$ is in general asymmetric w.r.t. the Δt-axis and the Δf-axis. This feature is a consequence of the non-stationary characteristics of the proposed channel model. We recall that a distinctive characteristic of a WSS random process is that its autocorrelation function is Hermitian symmetric [9, Theorem 10.12]. Nevertheless, from Fig. 2(b), one may note that $|R_H(t, f; \Delta t, \Delta f)|$ seems to become symmetric in the Δf (or Δt) variable as Δt (or Δf) approaches to zero. This behavior is more evident in Fig. 3, where we show the absolute value of $R_H(t, f; \Delta t, \Delta f)$ for the same observation point in the TF plane, and three different values of Δt (see Fig. 3(a)) and Δf (see Fig. 3(b)).

Figure 3(a) shows clearly that $|R_H(t, f; \Delta t, \Delta f)|$ becomes a symmetric function in the Δf variable as $\Delta t \to 0$. This was to be expected, since we discussed in the previous section that $H(t; f)$ can be modeled by a frequency-domain WSS random process if we neglect the channel's time selectivity. However, the graphs shown in Fig. 3(b) follow a trend that is somehow unexpected, as we concluded from (23) that under conditions of accelerated motion of the MSs, $H(t; f)$ does not fulfill the WSS condition in the time domain, even if the channel's frequency selectivity is neglected. A more in-depth inspection of the graph obtained for the case $\Delta f = 0$ reveals that $|R_H(t, f; \Delta t, \Delta f)|$ is in fact asymmetric, but the chosen observation window in the dimension of Δt is not large enough to make this characteristic readily apparent. To demonstrate that $|R_H(t, f; \Delta t, \Delta f)|$ is asymmetric in the Δt variable if $\Delta f = 0$, we have recomputed the aforementioned graph by making $T_0 = 2$ and $\Delta t \in [-1, 1]$. The results are presented in Fig. 4.

V. Conclusions

A novel GBSM for non-WSSUS M2M channels has been proposed in this paper. This new model takes into account the variations in velocity that the MSs may experience in reality while communicating with each other. Based on this model, we derived a general expression for the 4D TFCF of the channel. This expression provides a tractable baseline for investigating the non-stationary characteristics and stationarity regions of doubly-selective M2M fading channels under accelerated motion of the MSs. The preliminary results presented in this

$$\mathcal{A}(t, f; \Delta t, \Delta f) = \mathcal{Z}(t, f; \Delta t, \Delta f)\, F_c^T(t) + \mathcal{W}(t, f, \Delta t)\, \dot{f}_{\max}^T(\Delta t)\cos(\beta_T) - \Delta f\left(\frac{D + d}{\mathcal{C}}\right) \quad (27a)$$

$$\mathcal{B}_c(t, f; \Delta t, \Delta f) = \mathcal{Z}(t, f; \Delta t, \Delta f)\, F_c^R(t) + \mathcal{W}(t, f, \Delta t)\, \dot{f}_{\max}^R(\Delta t)\cos(\beta_R) + \Delta f\frac{d}{\mathcal{C}} \quad (27b)$$

$$\mathcal{B}_s(t, f; \Delta t, \Delta f) = \mathcal{Z}(t, f; \Delta t, \Delta f)\left[\frac{d}{D}F_s^T(t) + F_s^R(t)\right] + \mathcal{W}(t, f, \Delta t)\left[\frac{d}{D}\dot{f}_{\max}^T(\Delta t)\sin(\beta_T) + \dot{f}_{\max}^R(\Delta t)\sin(\beta_R)\right] \quad (27c)$$

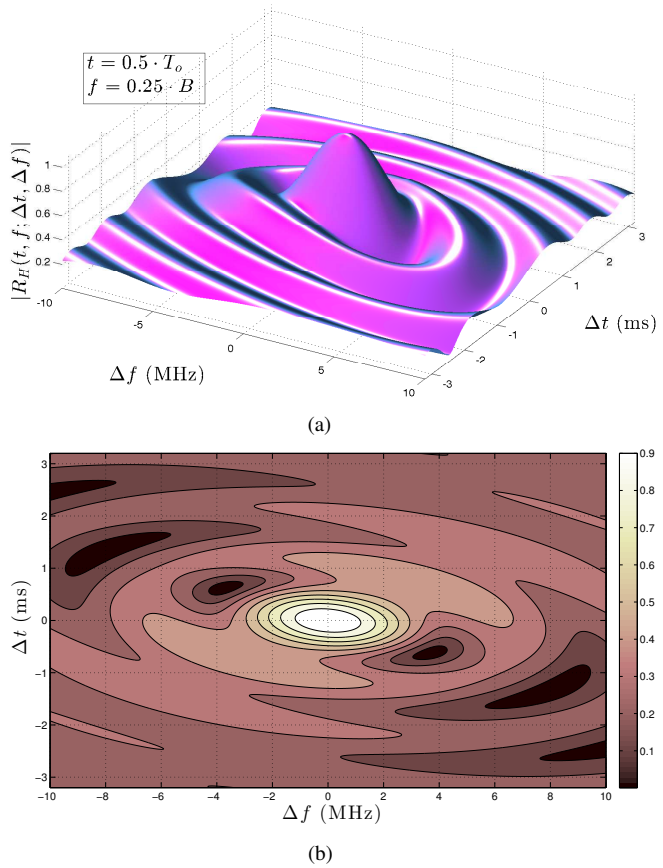

Fig. 2. The 4D TFCF $R_H(t, f; \Delta t, \Delta f)$ at $(t, f) = (0.5\,T_0, 0.25B)$: (a) Absolute value of $R_H(t, f; \Delta t, \Delta f)$, (b) Contour plot of $|R_H(t, f; \Delta t, \Delta f)|$ ($T_0 = 6.4$ ms, $B = 10$ MHz).

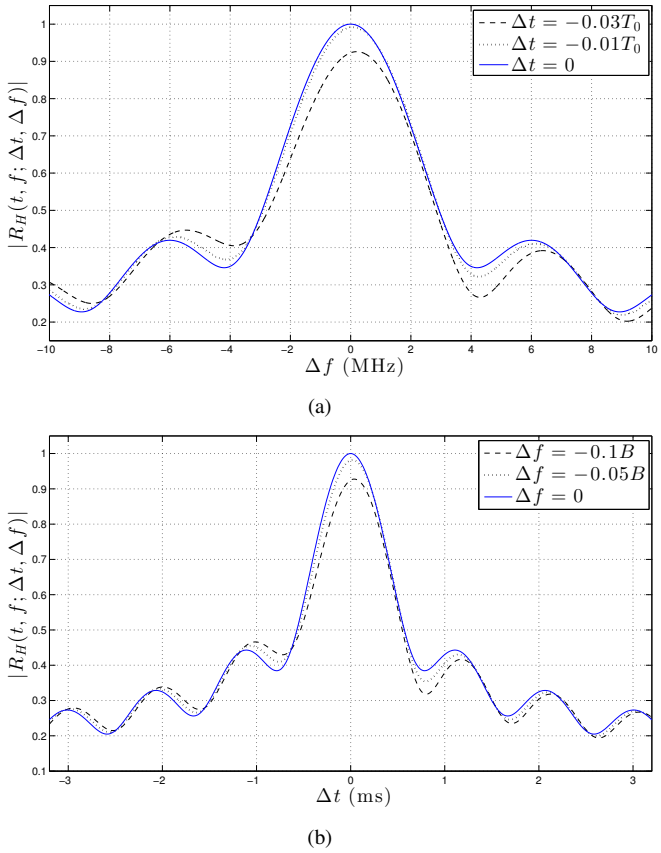

Fig. 3. Absolute value of the 4D TFCF $R_H(t, f; \Delta t, \Delta f)$ at $(t, f) = (0.5\,T_0, 0.25B)$ for (a) $\Delta t \in \{-0.03T_0, -0.01T_0, 0\}$, and (b) $\Delta f \in \{-0.1B, -0.05B, 0\}$ ($T_0 = 6.4$ ms, $B = 10$ MHz).

paper indicate that the acceleration exacerbates the channel's non-stationarities in both the time and the frequency domains, with stronger effects in the time domain.

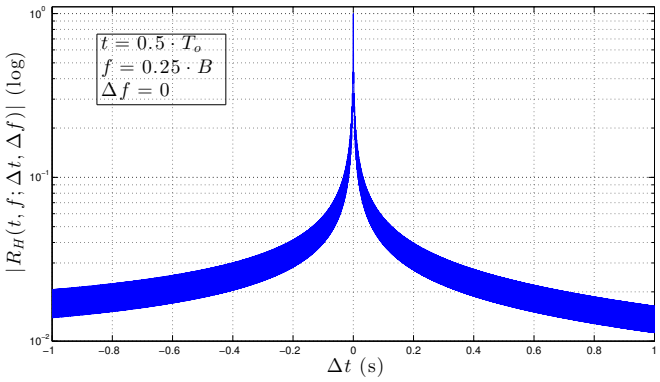

Fig. 4. Absolute value of the 4D TFCF $R_H(t, f; \Delta t, \Delta f)$ in log scale at $(t, f) = (0.5\,T_0, 0.25B)$ and $\Delta f = 0$ ($T_0 = 2$ s, $B = 10$ MHz).

References

[1] G. Karagiannis, O. Altintas, E. Ekici, G. Heijenk, B. Jarupan, K. Lin, and T. Weil, "Vehicular networking: A survey and tutorial on requirements, architectures, challenges, standards and solutions," *IEEE Communications Surveys & Tutorials*, vol. 13, no. 4, pp. 584–616, 2011.

[2] J. B. Kenney, "Dedicated short-range communications (DSRC) standards in the United States," *Proc. IEEE*, vol. 99, no. 7, pp. 1162–1182, Jul. 2011.

[3] J. Karedal, F. Tufvesson, N. Czink, A. Paier, C. Dumard, T. Zemen, C. Mecklenbräuker, and A. F. Molisch, "A geometry-based stochastic MIMO model for vehicle-to-vehicle communications," *IEEE Trans. Wireless Commun.*, vol. 8, no. 7, pp. 3646–3657, 2009.

[4] M. Walter, D. Shutin, and U.-C. Fiebig, "Delay-dependent Doppler probability density functions for vehicle-to-vehicle scatter channels," *IEEE Trans. Antennas Propag.*, vol. 62, no. 4, pp. 2238–2249, Apr. 2014.

[5] C. A. Gutiérrez, J. M. Luna-Rivera, and D. U. Campos-Delgado, "Modeling of non-stationary double-Rayleigh fading channels for mobile-to-mobile communications," in *Proc. 2016 European Wireless Conference (EW'2016)*, Oulu, Finland, 2016, pp. 131–136.

[6] C. A. Gutiérrez, J. T. Gutiérrez-Mena, J. M. Luna-Rivera, D. U. Campos-Delgado, R. Velazquez, and M. Pätzold, "Geometry-based statistical modeling of non-WSSUS mobile-to-mobile Rayleigh fading channels," under review.

[7] W. Dahech, M. Pätzold, and N. Youssef, "A non-stationary mobile-to-mobile multipath fading channel taking account of velocity variations of the mobile stations," in *Proc. 2015 9th European Conf. on Antennas and Propagation (EuCAP'15)*, Lisbon, Portugal, May 2015, pp. 1–4.

[8] B. Boashash, *Time Frequency Signal Analysis: A Comprehensive Reference*. Amsterdam: Elsevier, 2003.

[9] R. D. Yates and D. J. Goodman, *Probability and Stochastic Processes: A Friendly Introduction for Electrical and Computer Engineers*, 2nd ed. New Jersey: John Wiley and Sons, 2005.

[10] M. Pätzold, *Mobile Radio Channels*, 2nd ed. Chichester, UK: John Wiley and Sons, 2011.